Scripta Materialia 109 (2015) 23–27

Contents lists available at ScienceDirect

Scripta Materialia

journal homepage: www.elsevier.com/locate/scriptamat

Dynamic strain-induced transformation: An atomic scale investigation

H. Zhang [a,*], K.G. Pradeep [a,b,*], S. Mandal [a], D. Ponge [a], H. Springer [a], D. Raabe [a]

[a] Max-Planck Institut für Eisenforschung, Max-Planck Str 1, 40237 Düsseldorf, Germany
[b] Materials Chemistry, RWTH Aachen University, Kopernikusstr. 10, D-52074 Aachen, Germany

ARTICLE INFO

Article history:
Received 5 June 2015
Revised 7 July 2015
Accepted 8 July 2015
Available online 15 July 2015

Keywords:
Phase transformations
Nucleation
Thermodynamics
Diffusion
Three-dimensional atom probe (3DAP)

ABSTRACT

Phase transformations provide the most versatile access to the design of complex nanostructured alloys in terms of grain size, morphology, local chemical constitution etc. Here we study a special case of deformation induced phase transformation. More specifically, we investigate the atomistic mechanisms associated with dynamic strain-induced transformation (DSIT) in a dual-phased multicomponent iron-based alloy at high temperatures. DSIT phenomena and the associated secondary phase nucleation were observed at atomic scale using atom probe tomography. The obtained local chemical composition was used for simulating the nucleation process which revealed that DSIT, occurring during load exertion, proceeds by a diffusion-controlled nucleation process.

Grain refinement is an effective method for improving the mechanical properties of bulk structural materials. Two main routes exist to accomplish this: (1) severe plastic deformation, which can reduce the grain sizes down to even nanometers by inducing a high density of lattice defects; (2) mild plastic deformation in conjunction with tailored phase transformations resulting in a homogeneous distribution of micrometer-sized grains suitable for component design. In this context, the combined occurrence of deformation and phase transformation is of particular interest [1–7]. Here we address a specific case of dynamic strain-induced transformation (DSIT) in a Fe-based alloy occurring at 973 K where deformation assists phase transformation.

Previous studies have addressed the thermodynamic and kinetic aspects involved during DSIT [8–10]. The stored deformation energy (due to lattice distortion and defect accumulation) was an additional driving force for phase transformation in addition to the chemical free energy [8]. Hence, DSIT was considered as a nucleation dominant process [8,10]. However, these reports are mainly based on qualitative analysis and hence, the mechanism of DSIT is far from being completely understood. Essentially, even advanced techniques like in situ high energy X-ray diffraction fail in characterizing the nanometer-sized nuclei quantitatively [11]. In this study, we intend to explore the nucleation mechanisms of DSIT occurring at elevated temperatures by means of a quantitative technique with near-atomic resolution i.e. atom probe tomography (APT). Simulations based on classical nucleation theory, supported by thermodynamic phase predictions are conducted to correlate the actual elemental distribution across the nucleation sites as obtained using APT.

Hence, we follow a threefold strategy to investigate DIST: (i) capturing the onset of DSIT by interrupted deformation tests at low strain rates; (ii) stabilizing the strain-induced second phase nuclei immediately after DSIT onset; and (iii) avoiding subsequent phase transformations during cooling after DSIT. For this purpose we have designed a dual-phased alloy system consisting of a multicomponent ferrite matrix (body-centered cubic structure, bcc) and carbides (M_3C, orthorhombic structure, ort, volume fraction ~10%). The nominal composition of the alloy is Fe–5.6C–2.2Mn–3.3Si–1.1Cr–1.9Al (at.%). It should be noted that austenite phase (face-centered cubic structure, fcc) cannot be formed from such dual-phase system during isothermal annealing at 973 K (60 K below A_1-the equilibrium austenite transformation temperature). Nevertheless, austenite formation involving DSIT has been observed during 10^{-3} s^{-1} strain rate tensile testing at 973 K [12]. Such an observation indicates the contribution of deformation towards activating the non-equilibrium transformation. Owing to the multi-component alloying, the austenite speckles formed at the onset of DSIT are heavily alloyed with C, Mn and Cr, and hence are retained at room temperature (discussed later). Ferrite and carbides which are stable at lower temperatures (below A_1) do not undergo transformation during rapid cooling after DSIT at 80 K/s. Therefore, favorable

* Corresponding authors at: Max-Planck Institut für Eisenforschung, Max-Planck Str 1, 40237 Düsseldorf, Germany (H. Zhang, K.G. Pradeep).
E-mail addresses: h.zhang@mpie.de (H. Zhang), Pradeep@mch.rwth-aachen.de (K.G. Pradeep).

http://dx.doi.org/10.1016/j.scriptamat.2015.07.010
1359-6462/

preconditions are satisfied for capturing the austenite nucleation instance during the high temperature DSIT.

The DSIT nucleation was at first investigated using electron backscatter diffraction (EBSD) on a JEOL-6500F field-emission scanning electron microscope operated at 15 kV [13]. The obtained EBSD data (step size: 30 nm) was analyzed using the TSL OIM 6.2 analysis software. The elemental distribution and concentration across austenite nucleation sites were determined using APT with near-atomic resolution [14–16]. Considering the fact that the number density of austenite nucleation sites could be lower at the onset of DSIT, a series of needle-shaped APT specimens (providing dataset of 15 successful APT measurements containing at least 10 million atoms each with high reproducibility) were site-specifically prepared from the bulk sample using a dual-beam focused-ion-beam (FIB, FEI Helios Nanolab 600i) following the procedures described in [17]. The repetitive APT measurements not only increased the chances of obtaining the nucleation instance during DSIT but also statistically quantified the concentration of alloying elements adjacent to the nuclei. APT data collection was performed using a local electrode atom probe (LEAP™ 3000X HR, Cameca Instruments) in voltage mode at ~60 K. The pulse fraction and repetition rates were 15% and 200 kHz, respectively. Data reconstruction and analysis were carried out using IVAS 3.6.6 software. Based on the classical nucleation theory [18] that is modified according to diffusion kinetics and the quantitative APT results, thermodynamic predictions supporting the simulation of nucleation instance were performed using Thermocalc (TCFE7 database) [19].

Fig. 1a shows the EBSD phase map after the interrupted tensile test at ~250% strain. The combined image quality and high angle grain boundary (15–62.8°) notations reveal the existence of martensite (e.g. denoted by white arrows). The near-bcc martensitic structure with carbon oversaturation must have been transformed from austenite in a non-diffusional shear manner during rapid cooling after tensile deformation [12,20–22]. It therefore confirms that DSIT from ferrite to austenite has occurred at 973 K (60 K below Ae_1). Also, a small fraction of austenite formed at 973 K has not been transformed to martensite during cooling (retained austenite denoted in red color, some marked by yellow arrows in Fig. 1a). By performing such interrupted tensile tests at lower strains, it is understood that the DSIT process actually gets initiated at ~50% strain (Fig. 1b). Some austenite speckles (in several tens of nanometers, denoted by black arrows) have just nucleated along the periphery of carbides without undergoing significant growth. One such austenite nuclei (enclosed by yellow dotted rectangle in Fig. 1b) formed as a result of DSIT has been site-specifically lifted-out for APT measurements, the sequence of which has been shown in Fig. 1b–g. Prior to the final stage of FIB milling, the presence of carbide in the confined volume of APT tip was confirmed (dark contrast field within the white circle in Fig. 1f). Fig. 2a shows the three dimensional elemental distribution of only C and Al (for clarity) in an APT tip obtained from the sample deformed up to ~50% strain (i.e. Tip from the carbide dispersive area corresponding to Fig. 1b–g) [17]. By utilizing Al 0.5 at.% iso-concentration surface in the reconstructed volume, the presence of three chemically distinct regions can be observed (Fig. 2b). Specifically, two C enriched regions being separated from each other by an Al enriched interface (see Fig. 2c) are followed by an Al rich region. The concentration profile in Fig. 2b (taken along the cylindrical volume of $10 \times 10 \times 80\ nm^3$ as shown in Fig. 2a) further reveals that the Al rich zone has lower concentrations of C, Mn and Cr. This zone hence belongs to ferrite owing to its limited solubility for C, Mn and Cr. The higher concentration of Al in this zone could be attributed to the fact that Al is a bcc stabilizer [23]. The intermediate zone with the highest Mn concentration (~10 at.%) is austenite as Mn is a predominant fcc stabilizer [24]. The top-most region near the apex of the APT tip being enriched with C, Mn and Cr is that site-specifically prepared carbide phase observed in Fig. 1f [25]. In order to further confirm the chemical identity of different phases, several APT measurements have been performed along the carbide and ferrite grain boundaries. Such representative measurements for both these cases are shown in Fig. 2d–g. On one hand, Fig. 2d and e confirms the presence of carbide with composition identical to the tip apex carbide composition in Fig. 2a and b. Hence, the intermediate region in Fig. 2a having considerably enriched Mn concentration compared to that of the carbide at tip apex (~6 at.%, in Fig. 2b) can be confirmed as austenite. On the other hand, Fig. 2f and g indicates the segregation of C atoms (without any Al segregation) along the ferrite grain boundaries. Such an observation further confirms that Al atoms tend to segregate selectively along the phase boundaries of carbide and austenite (i.e. not at ferrite/carbide interfaces and ferrite grain boundaries). From the enlarged concentration profile of Al shown in Fig. 2c, a slight enrichment of Al due to its segregation along the carbide/austenite interface can be clearly observed. The enrichment of Mn in austenite region and segregation of Al at the carbide/austenite interface hints that substantial local atomic diffusion occurs during the nucleation of second phase upon DSIT.

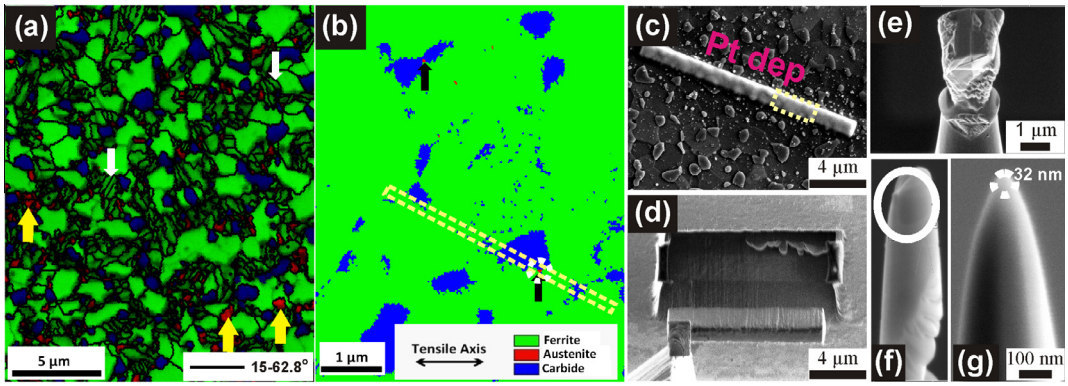

Fig. 1. (a) Phase plus image quality EBSD map of the specimen obtained after ~250% tensile strain at 973 K and $10^{-3}\ s^{-1}$ followed by rapid cooling at 80 K/s. Black lines show random high angle grain boundaries (15–62.8°). The zones with low image quality (e.g. marked by white arrows) represent martensite. Retained austenite is marked by yellow arrows (b) EBSD phase map of the specimen obtained after ~50% tensile strain at 973 K and $10^{-3}\ s^{-1}$ followed by rapid cooling at 80 K/s. Austenite speckles are indicated by black arrows. (c) SEM image of the specimen shown in (b) with a ~1 μm layer of Pt deposition for site specific lift-out. The yellow dotted rectangle in (c) corresponds with that in (b). (d) Pt deposited sample wedge being lifted-out using the nano-manipulator needle. (e) A sampled 2 μm wedge being deposited (using Pt precursor gas) onto a Si flat-top for APT needle preparation. The dark contrast field area within the solid white circle in (f) during FIB annular milling is carbide. (g) Final shape of ~32 nm diameter APT needle suitable for measurement. (For interpretation of the references to color in this figure legend, the reader is referred to the web version of this article.)